Soft Matter

PAPER

View Article Online
View Journal | View Issue

Cite this: *Soft Matter*, 2015, **11**, 2691

Molecular architecture requirements for polymer-grafted lignin superplasticizers†

Chetali Gupta,[a] Madeline J. Sverdlove[b] and Newell R. Washburn*[abc]

Superplasticizers are a class of anionic polymer dispersants used to inhibit aggregation in hydraulic cement, lowering the yield stress of cement pastes to improve workability and reduce water requirements. The plant-derived biopolymer lignin is commonly used as a low-cost/low-performance plasticizer, but attempts to improve its effects on cement rheology through copolymerization with synthetic monomers have not led to significant improvements. Here we demonstrate that kraft lignin can form the basis for high-performance superplasticizers in hydraulic cement, but the molecular architecture must be based on a lignin core with a synthetic-polymer corona that can be produced *via* controlled radical polymerization. Using slump tests of ordinary Portland cement pastes, we show that polyacrylamide-grafted lignin prepared *via* reversible addition-fragmentation chain transfer polymerization can reduce the yield stress of cement paste to similar levels as a leading commercial polycarboxylate ether superplasticizer at concentrations ten-fold lower, although the lignin material produced *via* controlled radical polymerization does not appear to reduce the dynamic viscosity of cement paste as effectively as the polycarboxylate superplasticizer, despite having a similar affinity for the individual mineral components of ordinary Portland cement. In contrast, polyacrylamide copolymerized with a methacrylated kraft lignin *via* conventional free radical polymerization having a similar overall composition did not reduce the yield stress or the viscosity of cement pastes. While further work is required to elucidate the mechanism of this effect, these results indicate that controlling the architecture of polymer-grafted lignin can significantly enhance its performance as a superplasticizer for cement.

Received 2nd December 2014
Accepted 10th February 2015

DOI: 10.1039/c4sm02675f

www.rsc.org/softmatter

1. Introduction

Ordinary Portland cement (OPC) is the largest-scale synthetic material manufactured,[1] with over 3.7 billion tons produced globally in 2012. It is based on four calcium aluminates and silicates that undergo a complex series of hydration reactions in which a colloidal gel intermediate forms involving aggregation and fusion of ceramic particles in an ionic medium.[2] A central challenge in cement technology is controlling the aggregation process during setting, which leads to a sharp increase in the yield stress of cement paste and reduces workability.[3,4]

Superplasticizers are a class of high-performance anionic polymers designed to modify the rheological properties of hydraulic cement.[5–7] Addition of a superplasticizer reduces the yield stress of cement paste and lowers water requirements. The leading commercial superplasticizer is based on a copolymer of acrylic acid and a poly(ethylene glycol) (PEG) acrylate.[8] Referred to as polycarboxylate ether (PCE), it has an anionic polymer backbone that adsorbs to ceramic particle surfaces, and the PEG side chains inhibit particle–particle aggregation through steric interactions at concentrations of 5 mg mL^{-1}.

Lignin is an aromatic biopolymer that is an important component of plants,[9] comprising 18% of corn stover and 20–30% of wood. Aliphatic hydroxyl and phenolic hydroxyl groups are the native reactive functional groups on lignin, but oxidation during processing can generate carboxylic acid moieties. One challenge facing the establishment of a robust biobased chemicals industry is developing large-scale technological applications for lignin, the main byproduct in cellulosic ethanol production.[10] While decomposition to aromatic chemical building blocks[11] and incorporation in commodity plastics[12] have been explored extensively, surfactant applications are currently the most widely used. Lignosulfonate, a lignin derivative produced from the sulfite pulping process, has a net negative charge and is broadly used as a low-cost/low-performance dispersant. In hydraulic cement, aluminates and other oxide constituents release hydroxide, resulting in particles with a net positive charge that are prone to aggregation that is strongly dependent on water content in the suspension. Lignosulfonates act as plasticizers for hydraulic cement, reducing water requirements by 5–10% by adsorbing to particle

[a]*Department of Materials Science & Engineering, Carnegie Mellon University, Pittsburgh, PA, USA. E-mail: washburn@andrew.cmu.edu*
[b]*Department of Chemistry, Carnegie Mellon University, Pittsburgh, PA, USA*
[c]*Department of Biomedical Engineering, Carnegie Mellon University, Pittsburgh, PA, USA*

† Electronic supplementary information (ESI) available. See DOI: 10.1039/c4sm02675f

surfaces and inhibiting aggregation through electrostatic repulsion.[13] However, lignosulfonates are known to have weak interfacial activities,[14–17] attributable to their disordered molecular structure.

To augment the plasticization effects of lignosulfonates, various hybrids of lignin and synthetic polymers have been investigated as potential superplasticizers for hydraulic cement. This architecture is based on copolymerization of lignin and synthetic monomers, either directly or by preparation of a reactive lignin derivative. For example, Ji *et al.* investigated sulphanilic acid–phenol–formaldehyde condensation polymers that incorporated lignosulfonate,[18] and formulations based on a methacrylated lignin derivative copolymerized with water-soluble acrylates have been patented.[19] However, both grafting approaches result in the formation of nanoscale crosslinked aggregates composed of synthetic polymer and lignin, and the effects on cement yield stress appear to be modest.[18]

Controlled radical polymerization from a lignin macroinitiator can be used to prepare a discrete grafted architecture composed of lignin cores with synthetic polymer coronas.[20,21] Previously we demonstrated that kraft lignin can be grafted with hydrophilic PAm using reversible addition-fragmentation chain transfer (RAFT) polymerization, and the resulting lignopolymer reduced aqueous surface tensions to as low as 52 mN m^{-1} and stabilized water-in-oil emulsions.[22] We postulated that these materials might be used as surfactants in a broad range of applications, but an important question centers on whether the CRP architecture offers any advantages over that prepared by conventional copolymerization strategies.

We present here a comparison of two polymer-grafted architectures based on kraft lignin and polyacrylamide and investigate their plasticization of cementitious suspensions. RAFT polymerization was used to graft acrylamide from a lignin macroinitiator whereas free radical polymerization (FRP) was used to copolymerize acrylamide with lignin functionalized by reacting with gylcidyl methacrylate (GM). These formulations were compared against a leading commercial PCE superplasticizer. We present comparative measurements of solution properties, and data on slump-spread measurements of yield stress, rheometer measurements of cement paste viscosity, and adsorption onto individual OPC mineral components. In addition, preliminary characterization of the compressive strength of hardened Portland cement is presented to investigate the effects of these admixtures on final material properties.

2. Experimental procedure

2.1. Materials and material preparation

Kraft lignin was purchased from TCI America having approximate molecular weight of 25 kDa was acidified prior to use. A commercial PCE (Adva 190) was generously provided by Grace Construction Chemicals and used as received.

RAFT was used to synthesize polymer-grafted kraft lignin *via* CRP following previously published procedures.[22] Briefly, the RAFT macroinitiator (0.1 g) along with AIBN (0.005 g, 0.03 mmol) was added to acrylamide (0.3 g, 4 mmol) in DMF (4 mL). The flask was then sealed with a rubber stopper and was degassed using N_2 for 30 min while stirring at room temperature and finally immersed in an oil bath at 70 °C. The solution was precipitated into hexanes, filtered, washed with CH_2Cl_2, and then placed under vacuum at 45 °C overnight.

For preparing the lignin-acrylamide copolymer *via* CRP, kraft lignin was first functionalized by reacting with GM through the epoxide ring. The lignin-GM macromonomer along with AIBN (0.005 g, 0.03 mmol) was added to acrylamide (0.3 g, 4 mmol) in DMF (4 mL). The flask was then sealed with a rubber stopper and was degassed using N_2 for 30 min while stirring at room temperature and finally immersed in an oil bath at 70 °C. Following polymerization for 1 h, the solution was precipitated into hexanes, filtered, washed with CH_2Cl_2, and then placed under vacuum at 45 °C overnight.

Individual mineral components of OPC were prepared through solid-state or sol–gel reactions. Dicalcium silicate (C_2S) powder was prepared by combining $CaCO_3$ and SiO_2 in stoichiometric amounts. The powder was ball milled for 24 hours and then calcined at 1500 °C for 24 hours. Tricalcium silicate (C_3S) powders were prepared using a sol–gel synthesis in which 0.5 mol of $Si(OC_2H_5)_4$ was mixed with 0.05 wt% of nitric acid as a catalyst which was then added to 200 mL of deionized water. Then 1.5 mol of $Ca(NO_3)_2 \cdot 4H_2O$ was subsequently added while stirring. The solution was then maintained at 60 °C until gelation occurred and then was dried at 120 °C for four hours. The final product was then calcined at 1450 °C for 8 hours.[23] Tetracalcium aluminoferrite (C_4AF) powders were synthesized by adding $CaCO_3$, Al_2O_3 (alumina) and Fe_2O_3 (iron(III) oxide) in stoichiometric amounts. The powder was ball milled for 24 hours and then calcined at 1350 °C for 24 hours. Tricalcium aluminate (C_3A) powders were synthesized using the modified Pechini method using $Ca(NO_3)_2 \cdot 4H_2O$ (26.239 g) and $(Al(NO_3)_3 \cdot 9H_2O$ (aluminium nitrate nonahydrate, 27.787 g)), which were dissolved in 45 mL of ethanol to obtain a CaO/Al_2O_3 molar ratio of 3. Citric acid was added such that molar ratio citric acid : total cations is 1 : 1. The mixture was stirred until a clear solution was obtained and then ethylene glycol was added to obtain a molar ratio of ethylene glycol : citric acid of 2 : 1. The solution was stirred at 80 °C for 24 h, until the formation of a viscous gel. The gel was then thermally treated at 150 °C for 24 h and formed a brown resin-type precursor. The precursor was calcined at 600 °C for 2 h and then 1300 °C for 4 h and 1350 °C for 1 h.[24] The final products for each phase were characterized using X-ray diffraction (X'Pert Pro MPD) using a continuous scan from 5° to 65° at a scan speed of 0.75° min^{-1}. Representative XRD plots are shown in ESI.†

2.2. Solution-properties measurements

Surface area for each phase was measured using the Brunauer–Emmett–Teller (BET) method using a Gemini VII Micrometrics surface area analyzer. Each sample was degassed for 24 hours at 60 °C prior to being analyzed.

Zeta potential and size distribution for each phase was measured in an aqueous solution at a concentration of 1 mg mL^{-1}. The zeta potential and particle diameter were measured using a Zeta-sizer (Malvern Instruments).

Adsorption of the different samples onto each cement phase was measured by analyzing the total amount of carbon left in the sample before and after adsorption. Each sample was mixed with the phase at 5 different concentrations (0.25, 0.5, 1, 2 and 4 mg mL^{-1}) for an hour and then centrifuged to obtain the top layer. The top layer was subsequently diluted and the total organic carbon content was measured using a GE InnovOX TOC analyzer.

2.3. Rheological and compressive strength measurements

Slump tests were used to gauge changes in yield stress of cement pastes. Samples were prepared using a Hobart mixer and were agitated for 3 minutes at a water-to-cement (w/c) ratio of 0.42 prior to being packed in a mini-slump cylinder, which was 3 cm in diameter. The cylinder was slowly lifted and diameters along two orthogonal directions were recorded and used to calculate the slump spread and relative flow area ratio. The slump height was also measured as an additional measure of cement flow.

Rheometric measurements on cement pastes were performed with a DHR Rheometer (TI Instruments) using a vane fixture to assess changes in paste viscosity. An oscillatory strain sweep was performed on the samples at a constant frequency of 1 Hz for samples with a w/c ratio of 0.42.

The compressive strength of each sample was tested at 7 days. Ten samples for each superplasticizer were tested and compared to OPC. The samples were prepare by adding 200 g of cement along with superplasticizers dissolved in water to create a 0.42 w/c ratio at 0.05 wt% polymer. The slurry was agitated using a Hobart mixer for three minutes and then poured into a $2'' \times 2''$ plastic mold from Deslauriers. The samples were allowed to cure for 7 days at room temperature and 100% humidity then tested on a Testmark CM-2500.

3. Results and discussion

3.1. Preparation of polymer-grafted lignin

In this work, lignin was grafted with PAm *via* RAFT and FRP as shown in Scheme 1. The lignin-based RAFT macroinitiator was prepared as previously described with initiator site density of 100 μmol per (g lignin) (approximately 2 per lignin particle) and an average degree of polymerization of 160, resulting in a product that was 60% lignin by mass.[22] For the comparable FRP material, lignin was reacted with GM to yield a similar initiator site density as the RAFT macroinitiator, and copolymerization of GM-lignin with acrylamide yielded a product postulated to resemble crosslinked nanogels synthesized through simultaneous polymerization of monofunctional and multifunctional monomers.[25] These reactions and products are depicted in Scheme 1.

For both functionalized lignin precursors, functionalization occurs at hydroxyl groups, but living polymerizations, such as RAFT, atom transfer radical polymerization,[20] or cationic ring-opening,[26] permit site-specific chain growth from the lignin macroinitiator, whereas FRP[27] or condensation polymerization[18] results in thermosets or crosslinked aggregates of lignin and synthetic polymer depending on reaction conditions. In this work, the RAFT macroinitiator, GM-lignin, and final products were characterized using ^{1}H NMR to establish average grafting density and degree of polymerization with pentafluorobenzaldehyde as an internal standard following previously reported methods[20] (see ESI†).

3.2. Solution properties

The characteristic sizes of these materials were measured using dynamic light scattering (DLS), and representative traces are shown in Fig. 1 along with the commercial PCE used for comparison. The RAFT-lignin-PAm had an average diameter of 35.9 nm at 0.25 mg mL^{-1} and a zeta potential of −36.2 mV. While the FRP-lignin-PAm had a similar zeta potential of −39.2 mV, the average diameter was 101.6 nm, consistent with the expected formation of a crosslinked aggregate of lignin and PAm. The commercial PCE had a diameter of 4.1 nm and a zeta potential of −48.9 mV, similar to previous studies.[28] Based on these data, schematic representations of both lignin products are shown in Fig. 1d. Also shown in Fig. 1 are solutions of each compound; the lignin solutions were clear and had a light brown color while the commercial PCE solution is dyed light green by the manufacturer.

3.3 Cement-paste rheology

To investigate the effects of lignin-PAm formulations on the rheological properties of hydraulic cement, slump tests were performed in comparison with neat OPC and OPC containing PCE at a w/c ratio of 0.42.[29,30] Slump tests are the most common measure of hydraulic cement rheology, and are an established first method of characterizing superplasticizers.[31] In these tests, cement paste is prepared using standardized mixing conditions and loaded into a metal cone[32] or cylinder,[29] which is raised to allow the cement to flow until the yield stress exceeds the shear stress. The experimental parameters recorded are the change in height and diameter from the original shape. While the complex phenomenon of cement flow is captured in only two geometric parameters, slump tests have the advantage of high levels of reproducibility when conditions are carefully controlled. Representative pictures of the slumps are shown in Fig. 2.

The slump spread as a function of superplasticizer concentration is presented in Fig. 3. When compared to commercial PCE, RAFT-lignin-PAm results in almost comparable increases in spread but performs much better at lower concentrations. At 0.025 wt%, the spread is anywhere from 20–30 mm larger than PCE or neat Portland cement. It is interesting to note that the slump spread is a more gradual function of RAFT lignin-PAm concentration whereas PCE experiences a steep increase at a concentration around 0.175%. In contrast, FRP lignin-PAm has very modest effects on the slump spread of OPC, suggesting this grafting architecture does not result in effective dispersants. The relative flow area ratio (Γ) was also calculated for each slump and results are reported in ESI.†

In slump tests, cement pastes flow until the yield stress exceeds the shear stress,[33] and analytical modeling provides a

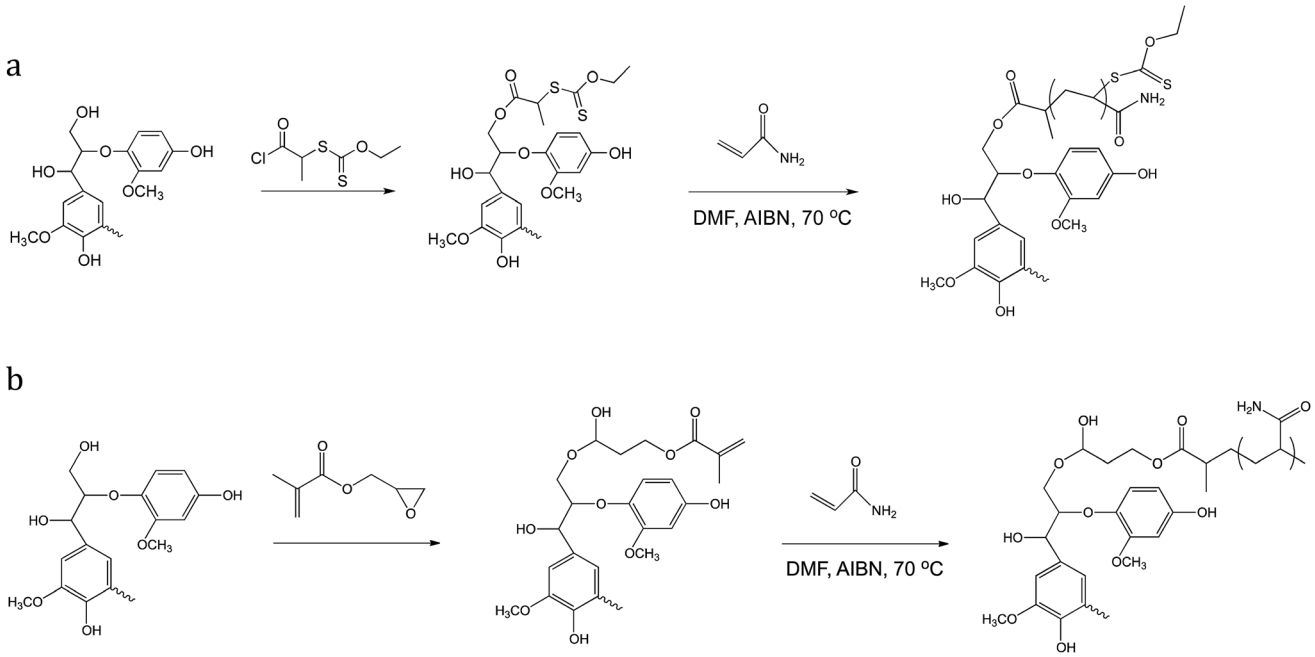

Scheme 1 Preparation of polymer-grafted lignin *via* (a) RAFT and (b) FRP.

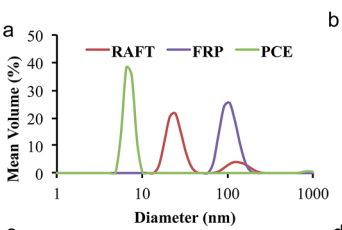

c

Sample (mg/mL)	Zeta Potential (mV)	Diameter (nm)
RAFT	-36.2 ± 0.6	35.9
FRP	-39.2 ± 0.9	101.6
PCE	-48.9 ± 0.7	6.5

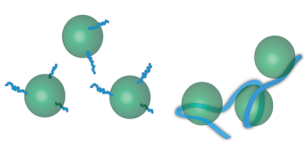

Fig. 1 (a) Polymer size characterization using DLS at a concentration of 0.25 mg mL^{-1}. (b) Picture of RAFT, FRP, and PCE solutions. (c) Table showing zeta potential and average diameter of superplasticizer solutions at a concentration of 0.25 mg mL^{-1}. (d) Schematics of RAFT (left) and FRP (right) products.

functional relationship between the slump spread R and the shear stress τ_0. When surface tension effects are ignored and an oblong initial geometry is assumed, the shear stress takes the form

$$\tau_0 = \frac{225\rho\, g\, V^2}{128\pi^2 R^5} \quad (1)$$

where ρ is the paste density, g is the gravitational constant, and V is the volume. Using this equation, the yield stress of OPC at w/c of 0.42 is calculated to be 236.3 ± 15.3 Pa while that containing 2.7 mg mL^{-1} of RAFT lignin-PAm was 31.8 ± 6.2 Pa compared to 20.6 ± 5.4 Pa for PCE at the same concentration. From these values it is concluded that even small increases in slump spread stem from significant decreases in yield stress.

To further investigate changes in rheological properties of cement pastes, oscillatory rheometry experiments were performed to measure changes in η' under a strain-magnitude sweep at a constant shear rate of 0.01 rad s^{-1} using a vane fixture to prevent slip at the rheometer interface.[34,35] These experiments were designed to probe the viscous response of cement pastes as the colloidal gel network was gradually disrupted under increasing oscillatory strain. The viscoelasticity of cement paste has been shown to depend strongly on the state of dispersion, with Newtonian behavior observed for higher w/c ratio and superplasticizer concentrations, but complex thixotropic behavior is observed otherwise.[34,36,37]

Fig. 4 shows η' for cement pastes (w/c = 0.42) at superplasticizer concentrations of 0.05 wt% and 0.1 wt%, which are near the transition at which PCE provided a significant increase in slump spread as a function of concentration. Shear thinning was observed for all formulations from oscillatory strains of 0.05–50%. At superplasticizer concentrations of 0.05 wt%, neat OPC had the highest viscosity at 0.05% strain at 581 Pa s, but the range of low-shear viscosity values was relatively low. In contrast, at 0.10 wt% superplasticizer, the cement paste containing FRP-lignin-PAm had a viscosity at 0.05% strain of 960 Pa s while that containing PCE had a value of 190 Pa s. Interestingly, the 0.05% strain viscosity for the RAFT-lignin-PAm sample had a value of 441 Pa s, much closer to that of neat OPC than the sample containing PCE. This suggests that while RAFT-lignin-PAm led to significant reductions in yield stress observed in slump tests, it had only modest effects on viscosity.

We propose that the discrepancy between the trends in yielding behavior measured in slump tests and the trends in

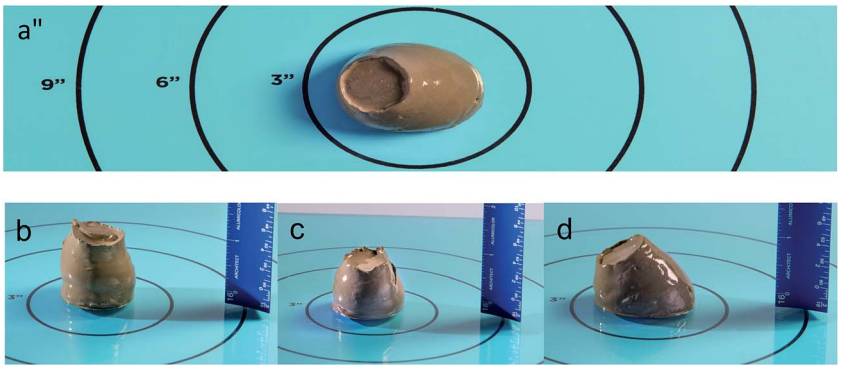

Fig. 2 Comparison of physical properties of cement with different superplasticizers. a, Enhanced view of the scale used for slump test with RAFT-lignin-PAm sample. b, Slump test at 0.42 *w/c* ratio showing diameter and height for Portland cement. c, PCE (0.05 wt%) and d, RAFT-lignin-*g*-PAm (0.05 wt%).

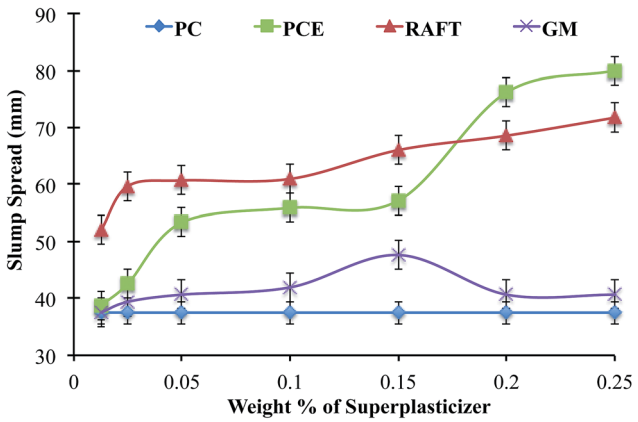

Fig. 3 Plot of slump spread for OPC as a function of superplasticizer concentration. All samples were prepared at 0.42 *w/c* ratio.

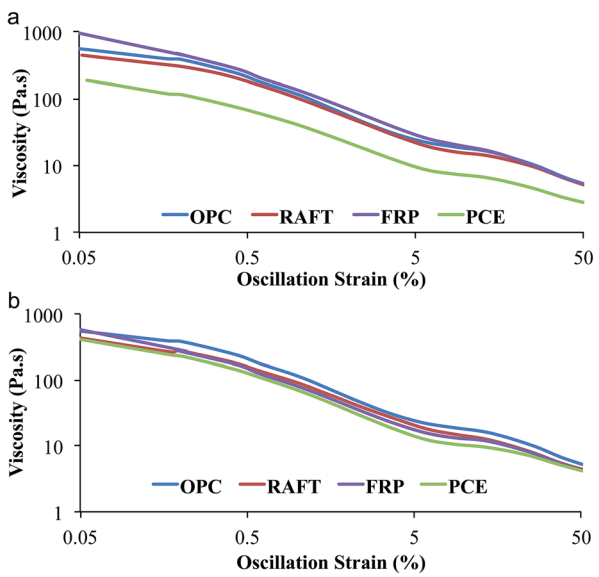

Fig. 4 Effect of superplasticizers on OPC viscosity (η') at (a) high concentration (0.1 wt%) and (b) low concentration (0.05 wt%), both with *w/c* ratio of 0.42.

viscous responses measured in rheometry tests are due to subtle differences in the nature of the dispersions in each formulation. Cement pastes containing PCE are highly dispersed at higher PCE concentrations,[38] resulting in reductions in both yield stress and viscosity, while FRP-lignin-PAm actually forms strongly bonded flocs due to its disorganized architecture containing multiple lignin particles, which can lead to increases in both yield stress and viscosity compared to neat cement pastes. In contrast, RAFT-lignin-PAm may induce the formation of weakly bonded flocs, which maintain the viscosity relative to neat cement pastes but have lower yield stress values and larger slump spreads.

The Krieger–Dougherty equation has been used to model the suspension viscosity η and can be used to evaluate aggregation phenomena.[39] Formally the equation models the dependence on particle volume fraction Φ and the maximum volume fraction Φ_M

$$\frac{\eta}{\eta_c} = \left(1 - \frac{\Phi}{\Phi_M}\right)^{-[\eta]\Phi_M} \quad (2)$$

where η_c is the viscosity of the continuous fluid phase (here assumed to be that of water), and $[\eta]$ is the intrinsic viscosity of the suspension. An intrinsic viscosity value of 2.5 is expected for suspensions of spherical particles, and departures from this are associated with crowding, flocculation, and coagulation. In studies on type I Portland cement paste at a *w/c* ratio of 0.32 and Φ_M of 0.64, the intrinsic viscosity was found to be a sensitive measure of dispersion, with $[\eta]$ ranging from 5.1 for dispersed samples containing a sulfonated naphthalene formaldehyde superplasticizer and 6.3 for flocculated samples without superplasticizer.[37]

To analyze the trends observed in Fig. 4, the viscosities were fit to the Krieger–Dougherty equation using a constant Φ_M value approximated to be 0.54 for both shear magnitudes,[40] which optimized the fit based on a Φ value of 0.51 calculated for a *w/c* ratio of 0.42, so that $[\eta]$ was the only free parameter. The viscous response tends to be considerably higher when flocculation occurs, so the low-strain data are expected to be a sensitive measure of aggregation, but all cement pastes should be more highly dispersed under higher oscillatory strains with lower

Table 1 Intrinsic viscosity values for different superplasticizers and concentrations at a constant Krieger–Dougherty Φ_M value of 0.54

	Intrinsic viscosity [η]			
	High strain (50.0%)		Low strain (0.05%)	
Sample	0.10 wt%	0.05 wt%	0.10 wt%	0.05 wt%
OPC	4.49	4.49	7.13	7.13
RAFT	4.43	4.40	6.91	6.93
FRP	4.51	4.39	7.32	7.16
PCE	4.28	4.40	6.50	6.87

instrinsic viscosity values. The results are shown in Table 1, with neat OPC having [η] of 7.13 and cement paste with 0.1 wt% PCE having [η] of 6.50 while the values with RAFT-lignin-PAm were slightly lower than that of neat OPC. In contrast, the intrinsic viscosities at 50.0% strain ranged from 4.28 for samples containing 0.10 wt% PCE to 4.51 for samples containing 0.10 wt% FRP-lignin-PAm. While this yields a range of intrinsic viscosity values that is higher than reported by Struble *et al.*,[37] the trend is consistent with the interpretation that while PCE functions by dispersing cement particles, RAFT-lignin-PAm results in the formation of weakly bonded flocs.

To gain insight into the interactions of these superplasticizers with cement particles, adsorption experiments were performed using individual OPC mineral components prepared and characterized in our labs (see ESI†), and the results are summarized in Fig. 5. Adsorption experiments were performed in 0.5% solutions of superplasticizer containing 5 wt% mineral, and results are reported as %superplasticizer adsorbed to each mineral phase normalized to the BET surface areas, which are included parenthetically in the figure caption. Zeta-potential measurements are also included for comparison; results from our measurements are consistent with literature values.[41,42]

OPC clinker is composed of the calcium silicates C_2S and C_3S, and the calcium aluminates C_3A and C_4AF. The silicates have weak anionic charge while the aluminates are cationic. Commercial superplasticizers have a negative charge that promotes avid adsorption to C_3A and C_4AF, but adsorption onto the silicate phases has been demonstrated,[43] which can be attributed in part to the high ionic strength (*ca.* 0.1 M)[44] of the cement fluid phase.

Three trends in the adsorption data are noted. The first is that PCE had the strongest adsorption across all phases, which is consistent with its high dispersant capabilities. The second is that FRP-lignin-PAm had comparable adsorption to aluminate phases as PCE but much weaker adsorption to silicate phases. The third is RAFT-lignin-PAm had adsorption affinity to silicate phases that was similar to PCE but this interaction with significantly weaker to aluminate phases, especially to C_4AF, which had the highest positive zeta potential in solution. However, commercial OPC generally has C_3S content ranging from 55–65%,[1] so effective interactions with this component are essential for superplasticizer function, and these were observed for RAFT-lignin-PAm.

The PCE and FRP-lignin-PAm trends essentially track with the polymer zeta potentials (−48.9 mV and −39.2 mV, respectively), although adsorption of the latter to the cationic aluminate phases was stronger than expected. However, the RAFT-lignin-PAm results are not predicted based on a zeta potential of −36.2 mV, with interactions with neutral/anionic silicate species being stronger than those of FRP-lignin-PAm but interactions with the highly cationic C_4AF significantly weaker. These trends point to lignin interactions that are not determined strictly by Coulombic forces between polymers and particle surfaces.

To provide a preliminary assessment of the effects of PAm-grafted kraft lignin on the setting process, compressive strengths were measured for samples at 7 days, the time point at which cement should exhibit basic structural characteristics. Lignosulfonates are known to retard the hydration reactions that occur in cement setting, and trade-offs are associated between fluidity and compressive strength with this class of

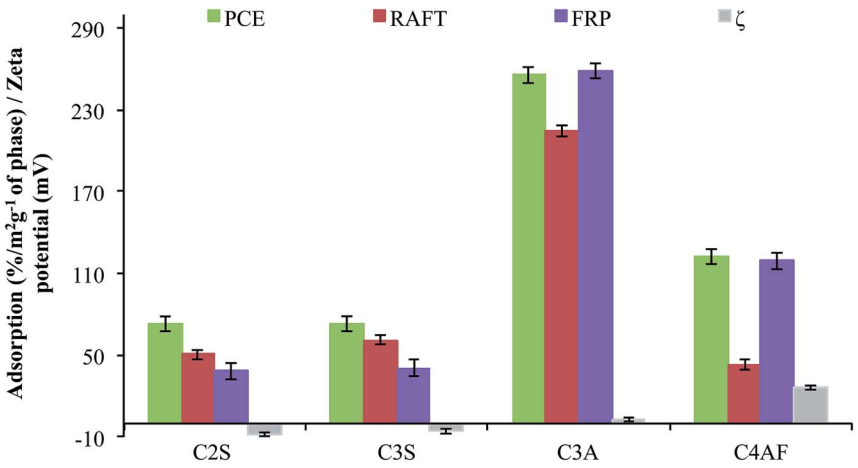

Fig. 5 Adsorption data for superplasticizers at different concentrations for cement phases normalized to the BET surface area of each mineral (reported parenthetically in $m^2\ g^{-1}$ along with the zeta potential value) (a) C_2S (BET = 0.9845 ± 0.0099 $m^2\ g^{-1}$; $\zeta = -5.96 \pm 0.42$ mV) (b) C_3S (BET = 0.8252 ± 0.0047 $m^2\ g^{-1}$; $\zeta = -7.77 \pm 0.32$ mV) (c) C_3A (BET = 0.3492 ± 0.0133 $m^2\ g^{-1}$; $\zeta = +3.23 \pm 0.44$ mV) (d) C_4AF (BET = 0.5797 ± 0.0017 $m^2\ g^{-1}$; $\zeta = +26.35 \pm 1.46$ mV).

lignin plasticizer.[13] The results are shown in Fig. 6, and the compressive strengths of samples containing at w/c ratio of 0.42 and containing 0.05% superplasticizers are all similar and 25% higher than for neat OPC. While more detailed tests of hydration and setting kinetics still need to be performed, these results suggest that RAFT-lignin-PAm does not interfere with these processes.

These results indicate that RAFT-lignin-PAm is an effective superplasticizer in reducing the yield stress of cement paste but it appears to have weak effects on the low-strain viscosity, whereas the leading commercial superplasticizer reduces both yield stress and low-strain viscosity. The yield stress calculated from the slump tests was 31.89 ± 2.5 Pa for cement paste with 0.1 wt% PCE and 20.64 ± 1.3 Pa for that containing 0.1 wt% RAFT-lignin-PAm. The stress applied to the vane fixture for these samples at 0.05% strain was of order 1 Pa and at 50.0% strain it was of order 10 Pa, so we conclude that the initial shear stress in the slump tests was sufficient to disrupt the aggregates with RAFT-lignin-PAm and set the viscosity to that of the disaggregated state, but the low-strain viscosities would differ due to fundamental differences in the microstructures.

The rheological characteristics of cement paste and fresh concrete are well described by the Herschel–Bulkley model: $\tau = \tau_0 + a\dot{\gamma}^n$,[45] which relates the applied stress τ to a yield stress τ_0 and the shear rate $\dot{\gamma}$. However, development of general microscopic models to describe this macroscopic material behavior has proved challenging. For non-reacting soft colloidal systems, a microscopic description can be based on a characteristic time t_B, which scales as the ratio of the solvent viscosity to the shear modulus (η_s/G_0) and accounts for dynamics based on the competition between elastic restoring forces and frictional motion between particles. For a paste composed of soft polymer microgels containing ionized acrylate groups, this model correctly predicts universal behavior of $\tau(\dot{\gamma})$ when the yield stress τ_0 was rescaled by t_B.[46] However, extending this model to cement pastes, which have a dynamic chemical evolution involving dissolution, gelation, and remineralization that provides an additional dimension of complexity,[47] is challenging, especially when trying to understand the additional effects of an organic dispersant.

The connections between aggregation strength and rheological parameters, such as yield stress and viscosity, have been studied for some time,[48] and this work has informed our basic understanding of these systems. In a simplest model, flocculating systems are assumed to form larger aggregates in which the total interaggregate bonding energy H_A is assumed scale with the particle–particle interaction energy of the constituent floc H_F and the ratio of the diameters of the constituent floc d_F to the aggregate diameter d_A as $H_A \sim H_F(d_A/d_F)$.[2]

Based on this physical model of aggregation, the Krieger–Dougherty equation predicts a divergence in the apparent viscosity as the volume fraction of solids Φ approaches the maximum value Φ_M.[39] At solids fractions that approach this limit asymptotically, there is an increase in the size of the aggregates that comprise the suspension and an associated divergence in the viscosity.

We propose that RAFT-lignin-PAm promotes the formation of weak aggregates in OPC at 0.42 w/c, which has a higher intrinsic viscosity than well dispersed suspensions containing PCE. In this simplest model, PCE could reduce both the particle–particle interaction energy H_F and the aggregate diameter d_A through steric effects of the PEG grafts, which would lead to an increase in slump spread and a decrease in viscosity relative to the values in neat cement paste. The RAFT-lignin-PAm may reduce H_F but result in a similar value for d_A, which would predict an increase in slump spread due to facile disruption of aggregates but impart a low-strain viscosity that is similar to that of neat cement paste. While ultimately the aggregate size distribution d_A is determined by the energetics of particle–particle interactions H_F, the molecular architecture of polymer-grafted lignin and how it interacts with the cementitious particle surfaces is thought to be the basis for the discrepancy between yield stress and viscosity trends. Comparisons with PCE superplasticizers may provide insight into how these lignin-based materials function.

The molecular basis for the differences in rheological properties between cement pastes containing PCE and RAFT-lignin-PAm stems from the differences in superplasticizer architecture, with PCE characterized as a linear polymer with a high density of grafted PEG side chains while RAFT-lignin-PAm has a more disorganized structure based on a lignin core and fewer pendant PAm chains. It may also be attributed to the complexities of kraft lignin chemistry based on aromatic, aliphatic, ether, hydroxyl, phenoxide, and carboxylate functionality.

The design principles for PCE superplasticizers are well understood,[49,50] with the copolymer being decomposed into n domains of N acrylic acid monomers containing one PEG side chain with degree of polymerization P per domain. Thus the degree of polymerization is $n \times N$ and the fraction of monomers with PEG side chains is $1/N$. Poly(acrylic acid) homopolymers have been shown to induce rapid setting of cement pastes,[5] presumably due to the strong affinity of carboxylate for Ca^{2+},[51] so that the polymer acts as a potent site of mineral aggregation and nucleation. The adsorption strength of PCE copolymers is balanced between promotion by the anionic groups and inhibition by the PEG side chains, and copolymers having short side chains (small P) with high concentration of ionic groups (large N) provide the greatest changes in particle zeta potentials,

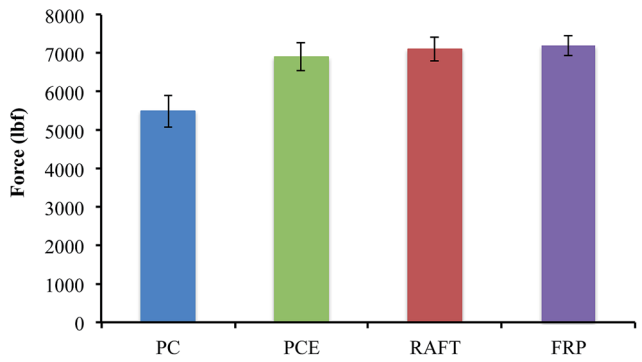

Fig. 6 Plot of 7 day compressive strength for Portland cement at 0.42 w/c ratio and 0.05 wt% of superplasticizer.

which can significantly contribute to the dispersant effects in tandem with steric interactions,[52,53] but the strongest dispersants appear to have a PEG degree of polymerization (P) of 20–50 and a backbone degree of polymerization ($n \times N$) of order 100. An additional variable that has been explored is the use of anionic monomers based on sulfonate *vs.* carboxylate groups. Many PCE formulations include ~10% sulfonate comonomers, which have improved dispersant power compared to formulations based strictly on acrylic acid. Polymer-grafted lignin has a similar rich parameter space, but the functional relationships between molecular parameters and properties, such as adsorption and dispersion, remain to be determined.

The preliminary investigation presented here focused on kraft lignin due to its good solubility in polar solvents that allow for facile RAFT polymerizations,[54] but this approach is being extended to lignosulfonates, which are already commonly used cement plasticizers and might work more effectively with grafted polymers and possibly more effectively than kraft lignin with carboxylate groups. Indeed, until the development of PCE, sulfonated polymers, such as sulfonated naphthalene formaldehyde condensate,[6] were the leading commercial superplasticizers, and lignosulfonate copolymerized in sulphanilic acid–phenol–formaldehyde condensate was reported to have improved plasticizing effects on cement paste.[18]

Controlled radical polymerization provides access to polymer-grafted lignin architectures that are distinct from those prepared by FRP or condensation polymerization. While this basic architecture appears to offer significant performance enhancements as a superplasticizer, questions remain on the optimal grafting density and length in cement applications. In addition, utilization of sulfonate or carboxylate monomers in the grafts could further tune interactions between ceramic particles and test whether the mechanism involves inducing the formation of weak flocs in cementitious suspensions. Grafting density is also expected to tune adsorption strength with a similar competition between charge density and polymer-graft density as observed in PCE.[49]

4. Conclusions

Our results demonstrate that high-performance dispersants are obtained through a grafted architecture using CRP of acrylamide from a lignin macroinitiator, whereas copolymerization of acrylamide with a functionalized lignin resulted in a nanogel that had similar particle size and charge but lacked the dispersant performance. Significant reductions in OPC yield stress are reported at lignopolymer concentrations 10-fold lower than a commercial PCE superplasticizer, but the viscosity of cement pastes containing PCE was still significantly lower than that containing RAFT-lignin-PAm. Trends in adsorption onto OPC mineral components indicate that the chemistry of kraft lignin influences the affinity of RAFT-lignin-PAm influences the affinity for cementitious particles compared to PCE, so that the plasticization mechanism is not based entirely on steric inhibition of aggregation, but further studies are necessary to elucidate the mechanism. Our results demonstrate that controlled radical polymerization chemistry is an essential tool in synthesizing technologically useful lignin-based superplasticizers, and these materials have excellent potential as a next-generation admixture for hydraulic cement.

Acknowledgements

The authors thank Prof. Larry Cartwright for assistance with compressive strength testing, Prof. Lynn Walker with rheology, and Mr Tim Kaulen for photography. Grace Construction Chemicals is acknowledged for providing Adva 190 and BASF is acknowledged for providing the mini slump cylinder used in this work. This work was supported by the Pennsylvania Department of Community and Economic Development through the Discovered in Pennsylvania, Developed in Pennsylvania (D2PA) Program.

References

1 P. K. Mehta and P. J. M. Monteiro, *Concrete: microstructure, properties, and materials*, McGraw-Hill, New York, 3rd edn, 2006.
2 J. W. Bullard, H. M. Jennings, R. A. Livingston, A. Nonat, G. W. Scherer, J. S. Schweitzer, K. L. Scrivener and J. J. Thomas, *Cem. Concr. Res.*, 2011, **41**, 1208–1223.
3 C. Jolicoeur and M. A. Simard, *Cem. Concr. Compos.*, 1998, **20**, 87–101.
4 N. Roussel and A. Gram, in *Simulation of fresh concrete flow: state-of-the art report of the Rilem Technical Committee 222-SCF*, 1st edn, 2014.
5 G. H. Kirby and J. A. Lewis, *J. Am. Ceram. Soc.*, 2004, **87**, 1643–1652.
6 R. J. Flatt and Y. F. Houst, *Cem. Concr. Res.*, 2001, **31**, 1169–1176.
7 R. J. Flatt, *Mater. Struct.*, 2004, **37**, 289–300.
8 K. Yamada, T. Takahashi, S. Hanehara and M. Matsuhisa, *Cem. Concr. Res.*, 2000, **30**, 197–207.
9 R. Vanholme, B. Demedts, K. Morreel, J. Ralph and W. Boerjan, *Plant Physiol.*, 2010, **153**, 895–905.
10 A. J. Ragauskas, G. T. Beckham, M. J. Biddy, R. Chandra, F. Chen, M. F. Davis, B. H. Davison, R. A. Dixon, P. Gilna, M. Keller, P. Langan, A. K. Naskar, J. N. Saddler, T. J. Tschaplinski, G. A. Tuskan and C. E. Wyman, *Science*, 2014, **344**, 709–718.
11 J. Zakzeski, P. C. A. Bruijnincx, A. L. Jongerius and B. M. Weckhuysen, *Chem. Rev.*, 2010, **110**, 3552–3599.
12 H. Chung and N. R. Washburn, *Green Mater.*, 2012, **1**, 137–160.
13 A. Y. A. Mollah, P. Palta, T. R. Hess, R. K. Vempati and D. L. Cocke, *Cem. Concr. Res.*, 1995, **25**, 671–682.
14 K. M. Askvik, S. A. Gundersen, J. Sjoblom, J. Merta and P. Stenius, *Colloids Surf., A*, 1999, **159**, 89–101.
15 S. A. Gundersen and J. Sjoblom, *Colloid Polym. Sci.*, 1999, **277**, 462–468.
16 D. Rana, G. H. Neale and V. Hornof, *Colloid Polym. Sci.*, 2002, **280**, 775–778.
17 V. Hornof and R. Hombek, *J. Appl. Polym. Sci.*, 1990, **41**, 2391–2398.

18 D. Ji, Z. Y. Luo, M. He, Y. J. Shi and X. L. Gu, *Cem. Concr. Res.*, 2012, **42**, 1199–1206.
19 T. Tomita, T. Hirata, *US Pat.* US7691982 B2, 2010.
20 S. L. Hilburg, A. N. Elder, H. Chung, R. Ferebee, M. R. Bockstaller and N. R. Washburn, *Polymer*, 2014, **55**, 995–1003.
21 Y. S. Kim and J. F. Kadla, *Biomacromolecules*, 2010, **11**, 981–988.
22 C. Gupta and N. R. Washburn, *Langmuir*, 2014, **30**, 9303–9312.
23 W. Y. Zhao and J. Chang, *Mater. Lett.*, 2004, **58**, 2350–2353.
24 G. Voicu, C. D. Ghitulica and E. Andronescu, *Mater. Charact.*, 2012, **73**, 89–95.
25 H. F. Gao and K. Matyjaszewski, *Prog. Polym. Sci.*, 2009, **34**, 317–350.
26 T. Nemoto, G. I. Konishi, Y. Tojo, Y. C. An and M. Funaoka, *J. Appl. Polym. Sci.*, 2012, **123**, 2636–2642.
27 J. F. Stanzione, P. A. Giangiulio, J. M. Sadler, J. J. La Scala and R. P. Wool, *ACS Sustainable Chem. Eng.*, 2013, **1**, 419–426.
28 L. R. Murray and K. A. Erk, *J. Appl. Polym. Sci.*, 2014, **131**, 40429.
29 N. Pashias, D. V. Boger, J. Summers and D. J. Glenister, *J. Rheol.*, 1996, **40**, 1179–1189.
30 N. Roussel and P. Coussot, *J. Rheol.*, 2005, **49**, 705–718.
31 ASTM, in *C494*.
32 J. Murata, *Mater. Struct.*, 1984, **98**, 117–129.
33 W. R. Schowalter and G. Christensen, *J. Rheol.*, 1998, **42**, 865–870.
34 J. E. Wallevik, *Cem. Concr. Res.*, 2009, **39**, 14–29.
35 H. A. Barnes and Q. D. Nguyen, *J. Non-Newtonian Fluid Mech.*, 2001, **98**, 1–14.
36 N. Roussel, G. Ovarlez, S. Garrault and C. Brumaud, *Cem. Concr. Res.*, 2012, **42**, 148–157.
37 L. Struble and G. K. Sun, *Adv. Cem. Based Mater.*, 1995, **2**, 62–69.
38 A. Ohta, T. Sugiyama and Y. Tanaka, *Am. Concr. Inst., SP*, 1997, **173**, 359–378.
39 G. N. Choi and I. M. Krieger, *J. Colloid Interface Sci.*, 1986, **113**, 101–113.
40 C. R. Wildemuth and M. C. Williams, *Rheol. Acta*, 1984, **23**, 627–635.
41 A. Zingg, F. Winnefeld, L. Holzer, J. Pakusch, S. Becker and L. Gauckler, *J. Colloid Interface Sci.*, 2008, **323**, 301–312.
42 E. Nagele, *Cem. Concr. Res.*, 1985, **15**, 453–462.
43 K. Yoshioka, E. Tazawa, K. Kawai and T. Enohata, *Cem. Concr. Res.*, 2002, **32**, 1507–1513.
44 M. Yang, C. M. Neubauer and H. M. Jennings, *Adv. Cem. Based Mater.*, 1997, **5**, 1–7.
45 F. de Larrard, C. F. Ferraris and T. Sedran, *Mater. Struct.*, 1998, **31**, 494–498.
46 M. Cloitre, R. Borrega, F. Monti and L. Leibler, *Phys. Rev. Lett.*, 2003, **90**, 068303.
47 N. Roussel, A. Lemaitre, R. J. Flatt and P. Coussot, *Cem. Concr. Res.*, 2010, **40**, 77–84.
48 A. S. Michaels and J. C. Bolger, *Ind. Eng. Chem. Fundam.*, 1962, **1**, 153–162.
49 D. Marchon, U. Sulser, A. Eberhardt and R. J. Flatt, *Soft Matter*, 2013, **9**, 10719–10728.
50 C. Gay and E. Raphael, *Adv. Colloid Interface Sci.*, 2001, **94**, 229–236.
51 J. Mattai and J. C. T. Kwak, *Macromolecules*, 1986, **19**, 1663–1667.
52 Q. P. Ran, P. Somasundaran, C. W. Miao, J. P. Liu, S. S. Wu and J. Shen, *J. Colloid Interface Sci.*, 2009, **336**, 624–633.
53 C. Z. Li, N. Q. Feng, Y. D. Li and R. J. Chen, *Cem. Concr. Res.*, 2005, **35**, 867–873.
54 J. Chiefari, Y. K. Chong, F. Ercole, J. Krstina, J. Jeffery, T. P. T. Le, R. T. A. Mayadunne, G. F. Meijs, C. L. Moad, G. Moad, E. Rizzardo and S. H. Thang, *Macromolecules*, 1998, **31**, 5559–5562.